BSGF - Earth Sciences Bulletin 2022, 193, 11
© M. Ouedraogo *et al.*, Published by EDP Sciences 2022
https://doi.org/10.1051/bsgf/2022009

BSGF
Earth Sciences Bulletin
Available online at:
www.bsgf.fr

OPEN ACCESS

Multifrequency electromagnetic method for the hydrogeophysical characterization of hard-rock aquifers: the case of the upstream watershed of White Bandama (northern Ivory Coast)

Moussa Ouedraogo[1,2,*], Marc Pessel[1], Véronique Durand[1], Albane Saintenoy[1], Bamory Kamagate[2,3] and Issiaka Savane[3]

[1] Université Paris-Saclay, CNRS, UMR 8148 GEOPS, 91405 Orsay cedex, France
[2] UFR Sciences Géologiques et Minières, Université de Man, BP 20, Man, Côte d'Ivoire
[3] Laboratoire de Géosciences et Environnement (LGE), Université Nangui Abrogoua, 02 BP 801, Abidjan 02, Côte d'Ivoire

Received: 15 May 2021 / Accepted: 3 June 2022 / Publishing online: 11 August 2022

Abstract – In West Africa, the drinking water supply relies on the hard-rock aquifers. In Ivory Coast, the population growth along with the climate changes make drinking water resources highly vulnerable. The White Bandama upstream watershed in northern Ivory Coast is located on a fissured hard-rock aquifer and is poorly known, both in the geometry of the reservoirs and in the hydrogeological potential of the reserves it contains. Indeed, the heterogeneous subsurface in this region shows high variability in the hydraulic conductivity inducing difficulties in the hydrogeological exploration. The determination of the geometry and hydrodynamic properties of the aquifer are required for a sustainable management of this water resource and for a better choice of future well locations. This study presents a hydrogeophysical approach using the multifrequency electromagnetic device PROMIS®, as well as lithology logs and geological information of a 30 × 30 km zone in the northwestern part of the White Bandama catchment. Our geophysical data are interpreted with 1D multi-layer models consistent with the discontinuities observed in lithology logs and the geology of the site. Results allow to precise the local thicknesses of the 3 main units of our study area down to 50 m, being from top to down, saprolite (which is often indured close to the surface), fissured-rock zone and rock substratum. Between the saprolite and the fissured zone, the main aquifer unit constitutes the interesting target for productive water wells. Its thickness ranges from 15 to 30 m. A detailed knowledge of the local aquifer geometry constitutes the first and crucial step before going further into a complete hydrogeological study.

Keywords: hard-rock aquifer / electromagnetic sounding / lithologs / hydrogeophysics / Ivory Coast

Résumé – Caractérisation hydrogéophysique des aquifères de socle par méthode électromagnétique multifréquentielle : cas du bassin versant du Bandama blanc amont (Nord de la Côte d'Ivoire). En Afrique de l'Ouest, l'on a recours aux aquifères de socle pour l'approvisionnement en eau potable. En Côte d'Ivoire, la croissance démographique et les changements climatiques rendent les ressources en eau potable très vulnérables. Le bassin versant du Bandama blanc amont, au Nord de la Côte d'Ivoire, est situé sur un aquifère de socle fissuré est mal connu, tant dans la géométrie des réservoirs que dans le potentiel hydrogéologique des réserves qu'il contient. En effet, le sous-sol hétérogène de cette région montre une forte variabilité de la conductivité hydraulique induisant des difficultés dans l'exploration hydrogéologique. La connaissance de la géométrie et des propriétés hydrodynamiques de l'aquifère est nécessaire pour une gestion durable de cette ressource en eau et pour un meilleur choix d'implantation des futurs forages d'eau potable. Cette étude présente une approche hydrogéophysique employant le dispositif électromagnétique multifréquenciel PROMIS®, ainsi que des logs de forages et des informations géologiques d'une zone de 30 x 30 km dans la partie Nord-ouest du bassin versant du Bandama blanc amont. Les données géophysiques sont interprétées avec des modèles multicouches 1D cohérents avec les discontinuités observées dans les coupes lithologiques et la géologie du site. Les résultats permettent de préciser les épaisseurs des 3 unités principales de notre zone d'étude jusqu'à 50 m, avec de haut en bas, la saprolite, une zone fissurée et le substratum rocheux. Entre la saprolite et la zone fissurée,

*Corresponding author: moussa.ouedraogo@univ-man.edu.ci

la principale unité aquifère constitue la cible intéressante pour les forages d'eau productifs. Son épaisseur varie de 15 à 30 m. Une connaissance détaillée de la géométrie locale de l'aquifère constitue la première étape cruciale avant d'aller plus loin dans une étude hydrogéologique complète.

Mots clés : aquifère de socle / sondage électromagnétique / lithologs / hydrogéophysique / Côte d'Ivoire

1 Introduction

The use of hard-rock aquifers as the main reliable source of drinking water for people living in rural Africa has grown considerably. Because of the intrinsic low hydraulic conductivity and low porosity of the basement rock, hard-rock aquifers are difficult for hydrogeological exploration, differ from other types of aquifers, and require technical knowledge to detect and extract significant quantities of water. The lack of sufficient knowledge on the flow and recharge of the groundwater in this type of aquifer has contributed to the unreasonable use of this resource (Chilton and Foster, 1995). However, significant progress has been made recently in the geological and hydrogeological characterization of these complex hard-rock aquifers (Dewandel *et al.*, 2006; Durand *et al.*, 2006; Lachassagne *et al.*, 2001; Lachassagne *et al.*, 2011; Vouillamoz *et al.*, 2014; Wyns *et al.*, 2004).

Lithology and tectonics control together (1) the nature and the thickness of the weathering, (2) the development of fractures, fault zones of vein structures and geological contacts, and (3) the presence of highly porous medium (Holland and Witthüser, 2011). Therefore, the characterization of the weathered layers geometry appears very important to identify the potentially productive reservoirs. They can be the targets of well fields for drinking water to supply the regions of high population densities with little or no alternative water sources.

The goal of the near-surface characterization is to delineate the weathered overburden and fracture zones in the study site with the intention of assessing the groundwater potential of the hard-rock aquifer. It aims consequently to locate optima points for sitting productive boreholes or dug wells in the study area.

In addition to the use of remote sensed methods, geomorphological and hydrogeological controls on the field, geophysical techniques are used to obtain information about the hydrologic characteristics of the weathered and fractured zones of the crystalline basement rocks, which relates to the occurrence of groundwater in the zones. Geophysical methods are commonly used for positioning boreholes in hard-rock aquifers, and most of hydraulic campaigns are based on common methods of electromagnetic (EM) and/or direct current resistivity measurements (Dutta *et al.*, 2006; Yadav and Singh, 2007). EM methods are ideally suited for hydrogeological investigations (McNeill, 1990). In particular, EM induction methods are widely used to determine the distribution of electrical resistivity and are well suited on the delineation of aquifers and clay layers because the EM field is strongly sensitive to electrically conductive material (Schamper *et al.*, 2012). Excellent resolution of the conductive targets make these methods a very attractive geophysical tool, with large investigation depth and rapid deployment at the sounding sites.

In this paper, we characterize a hard-rock aquifer geometry in a sub-Saharan context with multifrequency EM soundings (EMS) interpreted including information from local borehole lithological logs and geological observations. We apply this method to characterize and better understand the complexity of the hard-rock aquifer, which might help with the positioning of future highly productive water wells.

2 Study area

The White Bandama upstream watershed, in northern Ivory Coast, covers an area of 2,100 km^2 extending between 5°40' and 6°15' W longitude and 9°15' and 9°50' N latitude (Fig. 1). Its climate exerts a predominant influence on the various aspects of the basin natural environment. It is of Sudanese type and characterized by a dry season (November to May) and a rainy season (June to October), with annual average rainfall and temperature of, respectively, 1,332 mm and 26.7 °C, as measured at Korhogo weather station.

The geology of the study area is mainly represented by a succession of bands of Proterozoic crystalline rocks oriented NE–SW, whose ranges are dominated by granitoids, volcano-sedimentary of Birimian age (gabbros, schists, etc.). The observed geomorphic units are plateaus defining a peneplain altitude ranging from 200 to 400 m, and inselbergs up to 800 m. Two main tectonic faults are crossing the area.

We focus on a 30 × 30 km area SW of the White Bandama catchment presenting a uniform distribution of every distinct geological unit (Fig. 1). We have information from 30 existing boreholes, logged to get an integrated and detailed description of the aquifer. Fortunately, all boreholes drilled since 1994, due to Japanese Water Supply Project in Northern Ivory Coast, were registered in a national database. These boreholes were all made in the dry season to ensure the durability of the resource of water regardless of the season. Each borehole has a unique identity and position, technical specifications, information about the lithology and water chemistry. Their depth range from 41 m to 61 m. We accessed the detailed lithological logs (lithologs) that were prepared from drill cuttings by the French research office (BURGEAP), as well as the depth of water inflow. When possible, we measured the water level on each of them on the day of geophysical data acquisition. This water level is always at least 20 m above the recorded water inflow depth showing the aquifer is under pressure. In addition to these deep boreholes, it exists in the study area some shallow traditional hand dug wells in villages pumping water from the upper unconfined aquifer from depth between 9 and 16 m. The deep wells present high productivity, around 10 m^3/h, whereas the shallow ones deliver only 3 m^3/h.

3 Material and methods

3.1 The frequency-domain EM method

Several types of loop–loop frequency-domain EM systems are available for use in airborne (Sinha, 1990; Palacky and West, 1991), marine (Chave *et al.*, 1991) and ground-based surveys (Frischknecht *et al.*, 1991). Being very sensitive to

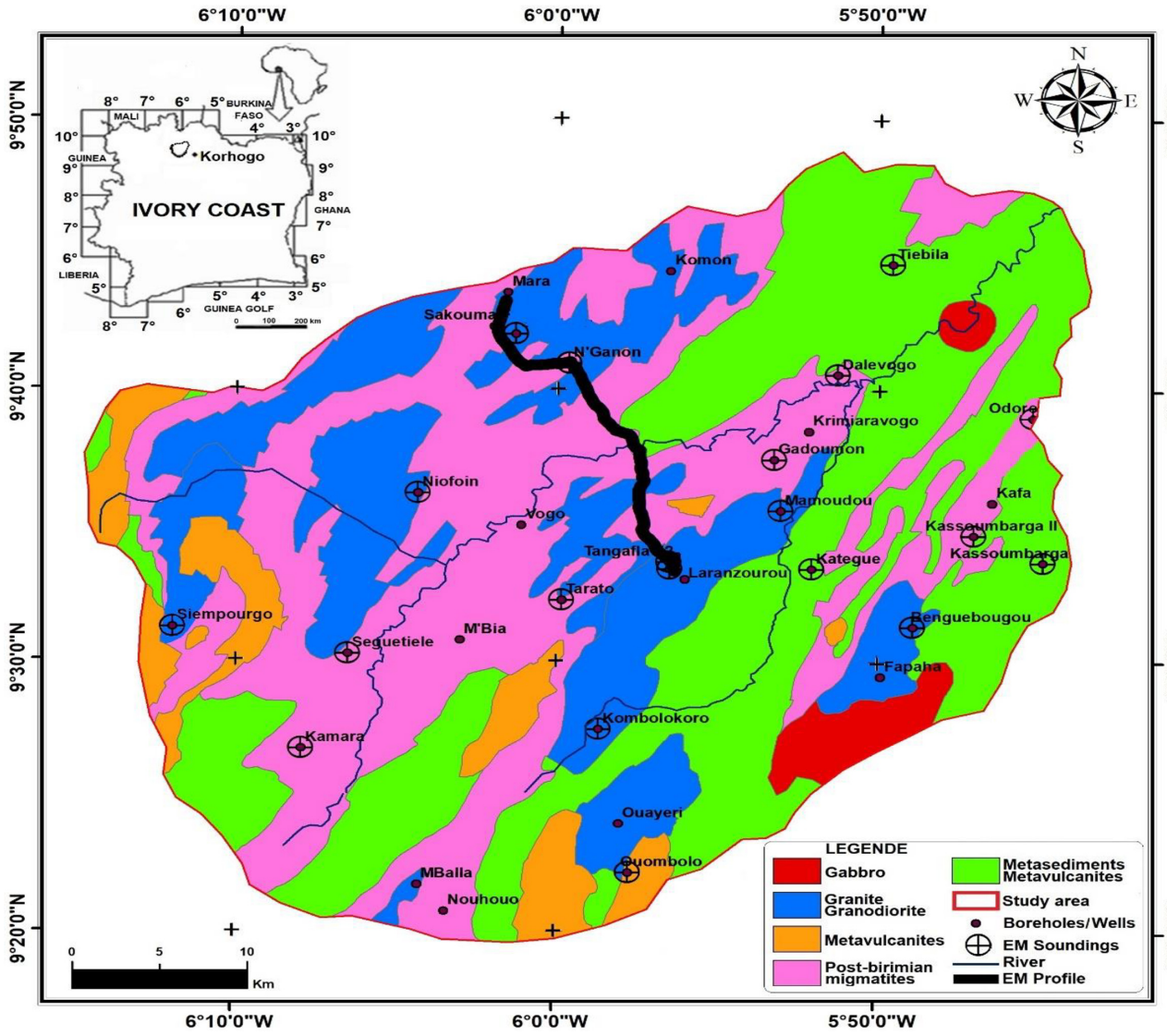

Fig. 1. Geological map of the White Bandama upstream watershed (simplified from Géomines, 1982) with the location of the survey area, observation wells, EMS and electromagnetic (EM) profile.

small changes in ground conductivity, the EM methods were developed as inductive survey techniques. They use two loops or coils to generate EM fields at selected frequencies (110, 220, 440, 880, 1,760, 3,520, 7,040, and 14,080 Hertz) and measure the resulting secondary magnetic field, from which the electrical properties of the ground are derived. The loops separation is chosen sufficiently large compared with the loop radius that the transmitter loop can be regarded as a magnetic dipole. Depending on the loop–loop geometry, we can measure distinct components of the ground response to a vertical or horizontal magnetic dipole source.

The primary field penetrates into the ground and induces eddy currents, particularly in electrically conductive elongated 2D targets, forming a secondary horizontal electric component in buried conductive structures (Tabbagh *et al.*, 1991). A secondary magnetic field is generated, which is out of phase with the primary magnetic field. The intensity of the secondary magnetic field depends on the conductivity of the ground (Khalil and Santos, 2010). Resultant magnetic field, which is produced by the interference between the primary and the secondary magnetic fields, is elliptically polarized. The parameters of interest are: (a) the orientation of the minor ellipse axis (tilt angle), also called the real (in-phase); and (b) the ratio of the minor to the major ellipse axes of polarization (ellipticity, e), also called the imaginary (quadrature) component (Karous and Hjelt, 1983).

Multifrequency EM method uses an EM field generated by the transmitter operating at some selected frequencies varying from 110 to 56,320 Hz. The PROMIS® (Iris Instruments) system allows measurements at 10 frequencies. Very little research measurements for ground imaging have been done with this quite recent equipment. One can find an analysis of 1D sensitivities (Schamper and Rejiba, 2011), a 1D inversion algorithm using multi-offset data and multi-component data (Schamper *et al.*, 2012), and 1D/2D inversion of ground constant offset loop–loop EM data (Guillemoteau *et al.*, 2015).

Multifrequency analysis of in-phase (IP) and out-of-phase (OP) data is commonly performed for the interpretation of

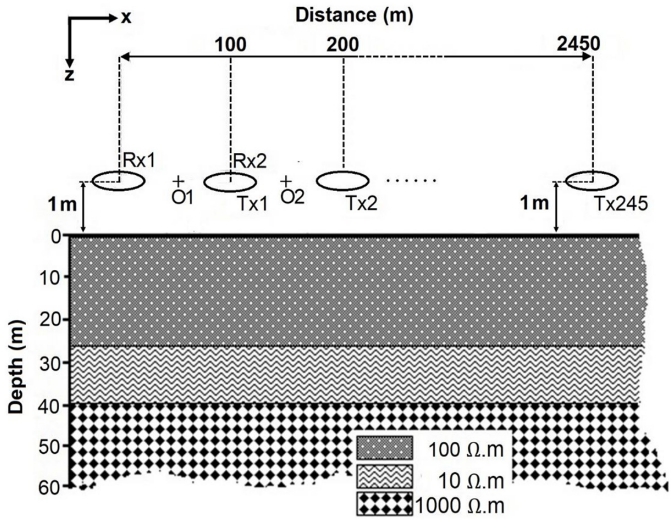

Fig. 2. Geometry of acquisition of the loop–loop horizontal coplanar (HCP) system used in our survey. The points O1 and O2 are the measured stations, at the middle between Tx and Rx.

airborne EM data (Beard and Nyquist, 1998; Farquharson *et al.*, 2003; Fraser, 1978; Huang and Fraser, 1996; Zhang *et al.*, 2000). Since multifrequency data are characterized by low and high induction numbers, both the IP and OP responses are affected by the electrical conductivity (Schamper *et al.*, 2012).

3.2 Multifrequency EM data

The PROMIS® (Iris Instruments) multifrequency electromagnetic method was used for hydrogeological investigations as it is sensitive to the aquifer lithology (clay mineral content), the pore-water content; and it allows the spatial distribution of these important hydrogeological features to be characterized. Its great advantage is to be easily deployed on large field areas. Nevertheless, it presents an extreme sensitivity to any artificial electromagnetic signal, as electric cables, vehicles or metallic structures; the chosen field site was therefore ideal for these type of constraints, as it is a rural area, with very few major equipments. In order to explore and map the aquifer of our region of interest, one 24.4 km-long profile consisting of 245 Electro-Magnetic Soundings (EMS), and additional 30 single EMS were acquired in February 2014 with a PROMIS®. Each EMS consists of 8 measurements acquired at 8 frequencies ranging from 110 to 14,080 Hz, setting the coils coplanar in the horizontal plane (HCP), with an offset $s = 100$ m. The profile, acquired in three days, ran from Tangafla to Mara in the SE to NW direction, perpendicularly to the direction of the geological structures and crossing the river (Fig. 1). Known drillings exist also along the profile. We collected additional 30 EMS centered on the deep boreholes disseminated across the area of interest.

Along the 24.4 km long profile, each EMS recorded every 100 m have been inverted to obtain smooth layer model which is similar to vertical electrical sounding (VES) data: a succession of vertical soundings along our profile whose inversion will provide a vertical distribution of the subsurface electrical resistivity. EMS data are inverted using the IX1D v3 software (Interpex, 2006), through an occam's inversion scheme.

Then a resistivity-depth model structure can be defined by a number of layers, resistivities and thicknesses for all the EMS as shown in Figure 2. The obtained data were analyzed and interpreted after their inversion using the IX1D v3 software. For every EMS, the layer model was obtained through an iterative process (1D inversion) which, in simple terms, results from minimizing the prediction and observation differences through an assessment of how well the suggested models fit the processed data. The inversions are one dimensional and are performed for each measurement independently.

4 Results and interpretation

The hydrogeological interpretation is superimposed on the resistivity distribution obtained through the inversion of acquired data, and is supported by field outcrop observations, borehole geological logs, geological maps and water-table measurements.

4.1 Electromagnetic soundings (EMS) interpretation

At each borehole location, as a first step, EMS data are inverted to obtain a smooth layer model down to 50 m (we use half Rx–Tx distance for the depth of investigation). The root mean square (RMS) error between the model response delivered from electrical resistivity models and our soundings data are ranging from 1.97% to 8.15%. We then invert again our data looking for a simpler model with a number of layers between 4 and 6 based on the smooth layer model obtained from the first EMS data inversion, and on the litholog of the boreholes. With the help of the latter models, we finally sum up our interpretation by setting a 3- to 4-layer model composed of saprolite (often composed of an indured subsurface horizon and a soft horizon underneath, lying in the saturated zone), fissured-rock and substratum.

We separated our results in three groups depending on the main lithology of the acquisition site.

In group 1, the EMS were carried out over granite substratum, in group 2, over schist substratum, and, in group 3, over post-birimian migmatites substratum. We present 3 interpreted EMS characteristic of group 1 in Figures 3–5, one from group 2 in Figure 6 and one from group 3 in Figure 7. In each of these figures, we present on the left side the lithologs obtained in the associated borehole. On the right, the smooth layer model in green, and the 4- to 6-layer interpreted layer model in red are shown. The vertical black arrows give the final 3-layer model summing up all these results.

According to the group 1, three typical layer models (6-layer model, 5-layer model and 4-layer model) were used to interpret the electromagnetic soundings in this study, as they fit the apparent resistivity data more reasonably.

A 6-layer model was used for the interpretation of apparent resistivities for Siempurgo EMS (Fig. 3), which layer 1 is composed of indured saprolite on the top surface with corresponding thickness of about 3.9 m. An underlying layer is delineated in this EMS with very low resistivities ranging from 10 to 90 Ω.m, and thickness of 6.1 m. This layer is thought to be composed mainly of clay, reached by hand dug wells for

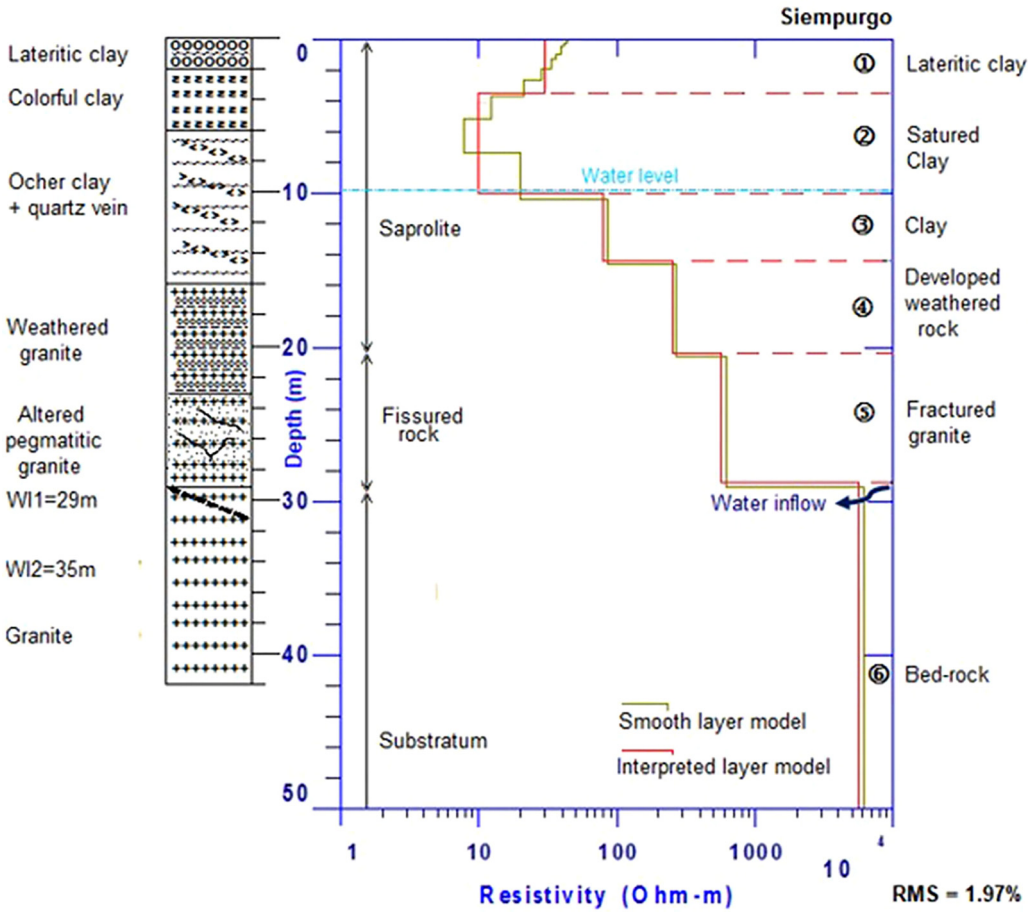

Fig. 3. Siempurgo granite site (group 1). Left: Litholog and observed water inflow (WI) depths. Right: EMS data inversion results (optimized smooth layer model in green, optimized 6-layer interpreted model in red).

water supply in the village. The resistivities and the thicknesses of the two following layers increase with depth, with respectively a consolidated clay layer (90 Ω.m; 4 m) overlying a thicker more resistive developed weathered granite (300 Ω.m, 6 m). At the depth of 20.2 m, appears the fifth layer which is more resistive and thicker (650 Ω.m; 9.3 m), and corresponds to the fractured granite, where water inflows deliver significant water yield. This layer is associated to the deeper aquifer reached by the borehole. A distinct very high resistive underlying layer of 5,500 Ω.m is associated to substratum, corresponding to the basement fresh granite. This model is given with a RMS error of 1.97%, and is declined in 3 main units with the saprolite unit composed by the first four layers, then the fissured-rock unit, and underlying substratum unit.

Figure 4 shows a 5-layer model with the same juxtaposition of layers, but regarding the EMS of Benguebougou site and distinguishing layers with their resistivities and respective thicknesses. From top to down, the saprolite unit is composed of indured lateritic clay layer (70 Ω.m; 6 m), a more conductive clayey sandy layer (10 to 110 Ω.m; 10 m) where hand dug wells are reached, and a more resistive layer (about 200 Ω.m, 8 m) corresponding to a weathered granite. This saprolite unit overlies the fissured-rock unit with the fissured and fractured granite at the depth of 23 m, with resistivity values around 900 Ω.m and a thickness of 10 m. This unit gives an important yield from the water inflows, due to its located fractures, and which are targets during the implementation of boreholes drilling. The last and third unit is the underlying substratum, consisting in granite bed-rock (about 900 Ω.m and more), which appears more and more solid and fresh with the depth. The RMS error given for this model is 3.67%.

Sakouma EMS (Fig. 5) is related to a 4-layer model from the group 1 over granite substratum, but in a relatively resistive context where the upper ferruginous indured saprolite layer looks like sand on the field. Thus, the saprolite unit is composed here by the upper consolidated sandy layer (60–105 Ω.m; 3.8 m), and a less resistive and thicker clayey sandy layer (20–90 Ω.m; 16.5 m). The water level is measured in this clayey sandy layer around the depth of 9 m, as shown by the located wells observed during the survey. This saprolite unit overlies the fissured-rock unit consisting in the fissured and fractured granite from around 21 m deep, with an active weathering giving by the way relative low resistivity values (around 160 Ω.m) and a thickness of 11 m. This layer appears to be the deeper aquifer recharged by the water inflows it contains, due to the fractures also targets of boreholes when

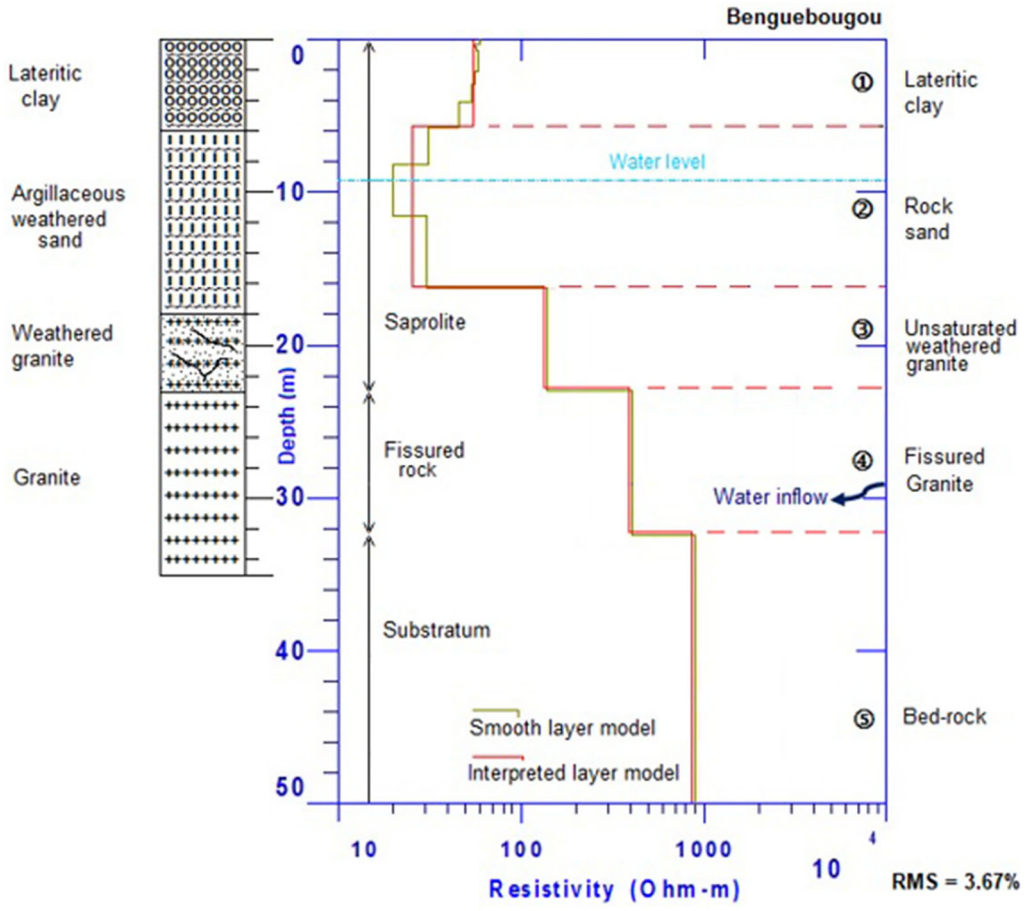

Fig. 4. Benguebougou granite site (group 1). Left: Litholog and observed water inflow (WI) depths. Right: EMS data inversion results (optimized smooth layer model in green, optimized 5-layer interpreted model in red).

drilling for water supply. The third unit is the underlying substratum, consisting in the relatively resistive and thicker granite bed-rock (410 Ω.m) due the weathering process that affected the ground at this place. The corresponding RMS error is estimated at 5.56% for this model that suits well lithostratigraphical information from Sakouma litholog.

The group 2 refers to the electromagnetic soundings conducted over schist or metasediments substratum. Thus, Gadoumon EMS (Fig. 6) allows highlighting a 5-layer model. From the top to down, the first layer is a thin and relative less resistive one of weakly indured lateritic clay (70–150 Ω.m, 3 m) that overlies a relative more resistive indured clay layer. The third layer is the least resistive and corresponds to a developed weathered schist (15–100 Ω.m; 6 m). These first layers sequence is associated to the upper saprolite unit.

At the depth of around 23 m and a thickness of about 9 m and more, the fissured-rock unit is mainly composed of the fractured schist layer that may be well located to catch the different water inflows from the fractures it contains. Finally, a distinct resistive layer with resistivity values around 1000 Ω.m is associated with the schist bed-rock, and constitutes the substratum in place. This model works also well with RMS error of 2.11 %, and also suits well with lithological and stratigraphical information given by Gadoumon litholog.

Finally, the group 3 concerns the EMS conducted over post-birimian migmatite substratum, as shown by Figure 7 regarding a 5-layer model from Odoro site. From surface to bottom it consists of: (1) a first layer of about 7.5 m, with resistivity ranging between 90 and 16 Ω.m, associated with the indured lateritic clay; (2) a more conductive layer with a thickness of 12.1 m. This second layer corresponds to argillaceous rock sand layer saturated in water, and where the water level was measured at 8 m down from the top surface; (3) a third more conductive layer (200 Ω.m; m) located at a depth of 20 m. This layers' sequence is the saprolite unit from top to a depth of 28 m. The fissured-rock unit is mainly composed of (4) the fractured migmatite relatively more resistive layer, but where water inflows corresponding to fractures are targets to deliver significant yield to the boreholes when drilling. The underlying unit is the substratum layer consisting in the (5) fresh and solid migmatite bed-rock, with very high resistivity (4,500 Ω.m). This model works also well with EMS error value of 2.93%, and suits well the lithostratigraphical information from Odoro litholog.

In general, the water level measured during geophysical investigations lies less than 10 m below the ground surface. Around 10 to 15 m deep, layers of lower resistivities (from 10 to 100 Ω.m), 6 to 8 m thick, forming the upper aquifer in which

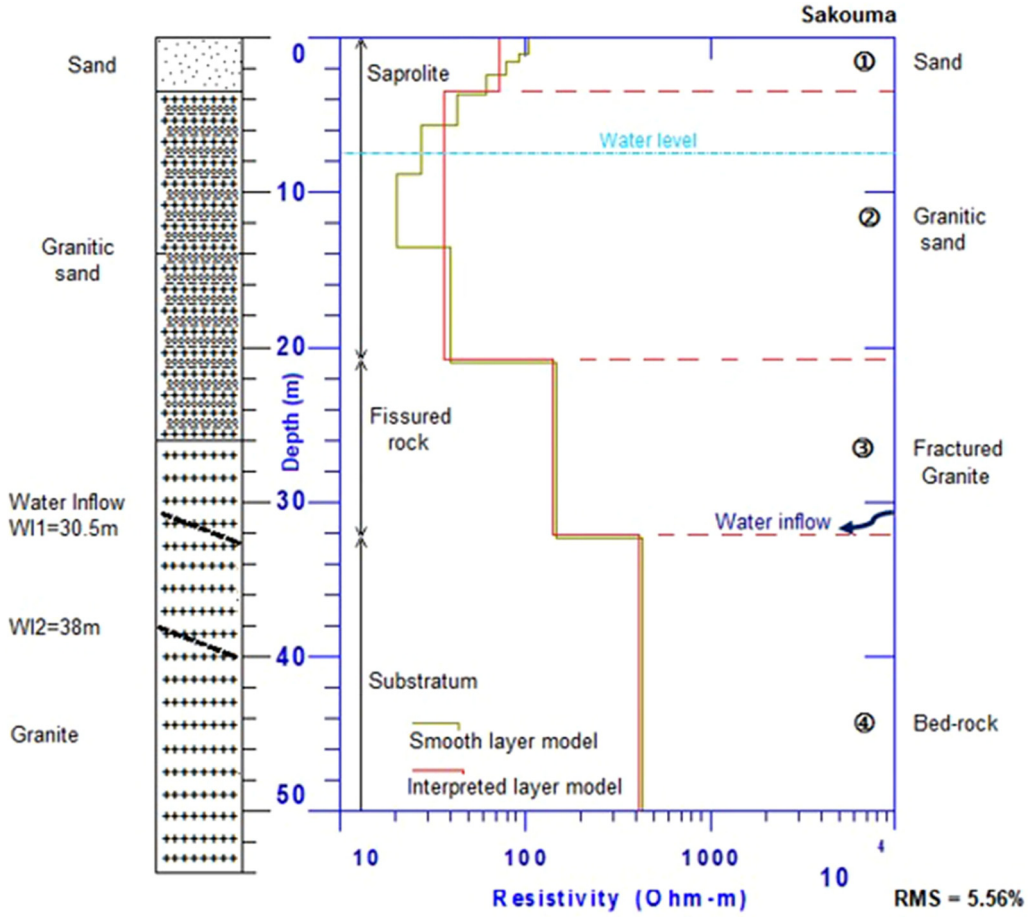

Fig. 5. Sakouma granite site (group 1). Left: Litholog and observed water inflow (WI) depths. Right: EMS data inversion results (optimized smooth layer model in green, optimized 4-layer interpreted model in red).

village wells are dug. At deeper depths (around 30 to 40 m), water inflows occur in layers of relatively higher resistivity (more than 550 Ω.m), reflecting the presence of fractures in hard-rock, and defining a deep-water aquifer under pressure, from 8 to 15 m thick and captured by boreholes. This can be correlated in groups 1, 2 and 3 (Figs. 3–7) to a zone of fissured-rock which thickness is decided from the interpreted thick-layer model (in red) and the water inflow depths. In these three groups, the lithologs indicate a fissured-rock zone overlying the substratum.

The electrical resistivity always increases with depth. But it is noticeable that some areas have very high surface resistivities due to indurated lateritic or ferruginous crust exceeding 10 m thick in some places.

4.2 2D profile interpretation

Figure 8 presents the pseudo 2D resistivity section of the 245 1D soundings along the study profile. This pseudo 2D resistivity section shows lateral and vertical variability of the geological structures apparent resistivity, correlated to lithology heterogeneity. As for the punctual data, the section shows the three main characteristic horizons from top to bottom: saprolite, fissured-rock and substratum. The first upper horizon is more or less resistive and its thickness varies from 10 to 30 m. The saprolite horizon shows much more conductive properties, with thickness between 15 and 30 m. The substratum underneath the two first layers shows the highest resistivity values.

In detail, the saprolite shows apparent resistivity values ranging from a few tens of Ω.m corresponding to top soil, lateritic clays, to more than 1,000 Ω.m in lateritic or ferralitic developed indured saprolite layer. This indured saprolite layer of 1 to 10 m thick or more, results from the recrystallization of goethite grains to massive hematite, at the top of the profile.

Over post-birimian migmatites, this upper horizon shows the highest apparent resistivity values between 2.5–5 km, 7.2–8.2 km, 10.6–11.3 km and 16.7–21.5 km on the profile. They are essentially battleships, indurated lateritic cuirass zones developed over several meters thick. Apparent resistivity is also high over granites but to a lesser degree compared to post-birimian migmatites. On the other hand, the apparent resistivity is lower over metasediments. These differences in apparent resistivity and corresponding lithology observed at the surface are due to the geological terrains nature, on the one hand, and, on the other hand, to the degree of weathering which affected them. The most conductive zones are those of geological formations that have undergone a more active

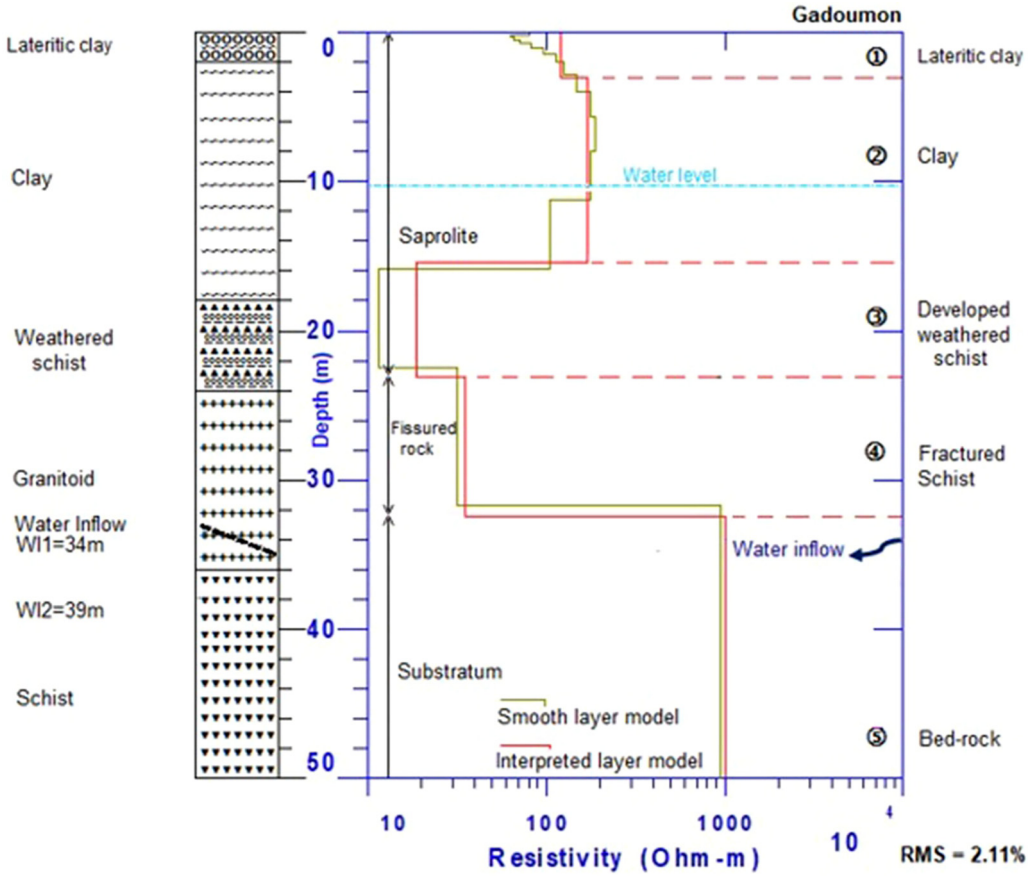

Fig. 6. Gadoumon schist site (group 2). Left: Litholog and observed water inflow (WI) depths. Right: EMS data inversion results (optimized smooth layer model in green, optimized 5-layer interpreted model in red).

weathering. This is the case of granites between 0.5–1.5 km and 21.4–23 km, where the cuirass is absent or stripped, with apparent resistivities of 100 to 500 Ω.m.

The second horizon is much more conductive, with apparent resistivity values ranging between 10 and 100 Ω.m or more. With depth, the primary rock remains hard and unweathered except along fractures and associated capillaries. This fissured zone highlights an aquifer layer of variable thickness, and is continuous in the first half part of the profile up to 14 km. Then, on the remaining part of the profile, this horizon appears more resistive, discontinuous, of greater thickness and becomes deeper. The second horizon is full of weathered formations, arenas, quartz veins, fractured and fissured-rocks. The clay contents in the upper part are important. Locally, areas of lower apparent resistivity that affect the rock from top to down, may correspond to vertical or subvertical fracture zones, or geological contacts, as it is the case between granite and post-birimian migmatites at 2.5 km; 5 km; 16.5 km; and at 21.5 km, on the one hand, and, on the other hand, between post-birimian migmatite and metasediments at 8.2 km; 10.6 km and at 12.1 km, and also the Bandama River fault at 9.9 km on profile. These are the aquifer recharge points and are targets for the implementation of high yield boreholes. In comparison with the geological map, the positions of the different geological contacts identified are corrected and given with much more precision by the resistivity section obtained. Some geological contacts correspond exactly to their position, while others are shifted from a few tens to hundreds of meters.

The second horizon is well located between an upper limit corresponding to the base of the lateritic indured saprolite layer, and a lower limit corresponding the top of the resistive sustratum layer. These two boundaries are irregular and define the thickness of the aquifer that is clearly distinguishable in the first half part of the profile.

The third horizon is the bedrock underlying the saprolite and the fissured zone. It is the most resistive horizon due to the rock nature and its very low weathering and fracturing degree. The basement depth also depends on the rock nature and the upper layers weathering degree. Thus, over the granite where the weathering is less active, the basement is shallower and is visible at less than 25 m from the ground in some places. On the other hand, over the post-birimian migmatites, where the weathering is very active, the basement plunges deeply and is not reached sometimes on the profile (more than 70 m deep).

In general, across this profile about 25 km long, a very wide distribution in resistivity values was observed ranging from 10–100 Ω.m up to 1,000 Ω.m and strongly related to the variety of the geological units investigated.

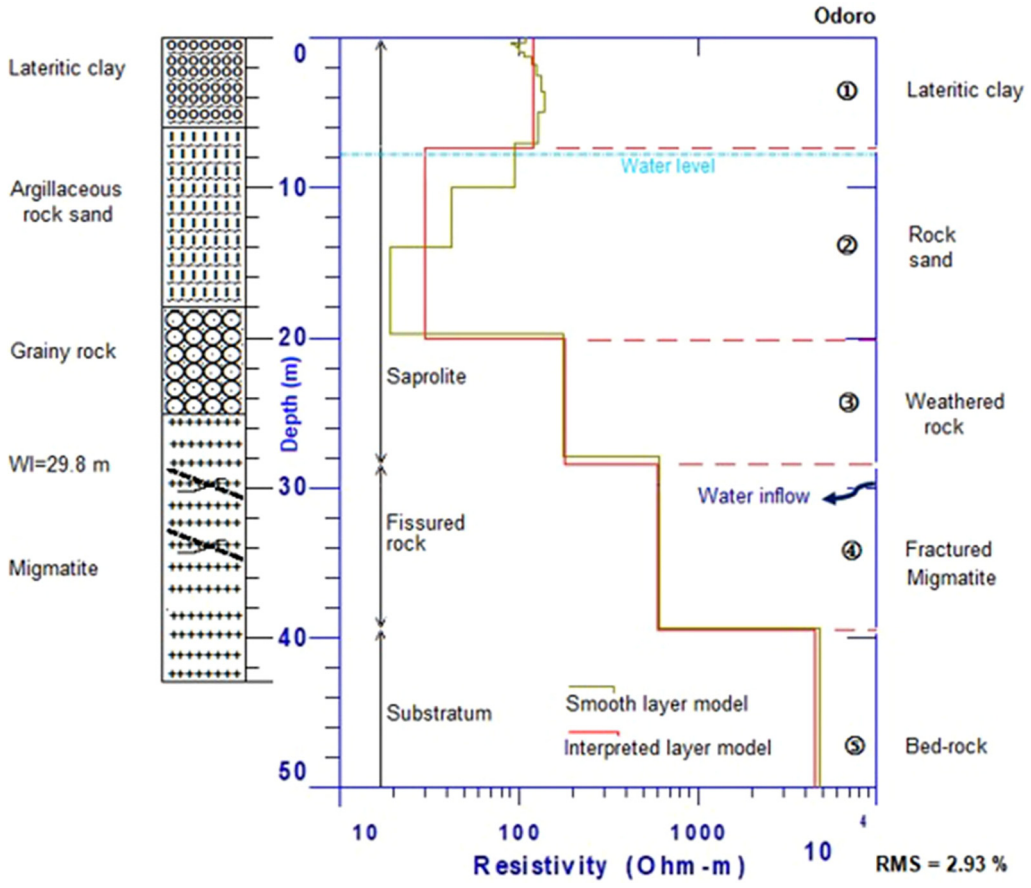

Fig. 7. Odoro Migmatite site (group 3). Left: Litholog and observed water inflow (WI) depths. Right: EMS data inversion results (optimized smooth layer model in green, optimized 5-layer interpreted model in red).

Different units of contrasting resistivity are visible. To the South-east a relatively low resistivity unit (40 to about 200 Ω.m) is clearly visible between two relatively high resistivity units (100 to >1,000 Ω.m) with some contact zones. Along the profile and from top to down, resistivity distribution is clearly dominated by a compartmentalization in three juxtaposed major units (saprolite, fissured zone, and substratum). Relatively high apparent resistivities (from about 1,000 Ω.m to more) on geological settings reflect the granite and post-birimian migmatite formations between Tangafla and Issoukaha villages, between NGanon and Sakouma villages, on one hand, and also around Mara village, whereas intermediate resistivity values (100 to 1,000 Ω.m) are observed in the central part around the Bandama stream on schist or metasediments formations, on some granite structure where the lateritic or ferruginous crust on the surface is absent.

We superposed on this profile information obtained from the area geology. In particular, we note the locations of different contact zones observed at the surface. These contacts as well as the faults are located on the geological map of the area, but our resistivity section gives more precision on the locations of these faults and contact zones. The Bandama stream is crossed at 10 km. In addition to the five villages (Tangafla, Issoukaha, NGanon, Sakouma and Mara), the profile crosses some seasonally flooded zones with rice crop as well as one sand pit.

The saprolite layer presents many variations in its electrical resistivity, with lower values at the two geological contacts as well as the tectonic faults, the river, the seasonally flooded area and the sand pit. The lower resistivity zones (blue in Fig. 8) are interpreted as some water infiltration areas that might be some recharge possibility for the fissured-rock zone.

5 Discussion

The electromagnetic soundings (EMS) data were interpreted at two levels: (1) a submetric scale corresponding to the smooth layer models resulting from EMS data inversion alone, (2) a simplified decametric scale model giving three layers: saprolite (including indured and soft saprolite), fissured layer and basement rock resulting from the interpretation of lithologs, geology of the area and water inflow depth. Except for the indured saprolite layer, the distinction of three layers is a usual conceptual model of hard-rock aquifer obtained in India by Ahmed *et al.* (1995), in France by Lachassagne *et al.* (2001) and Wyns *et al.* (2004) using magnetic resonance sounding (MRS) method coupled with geometrical aquifer modeling.

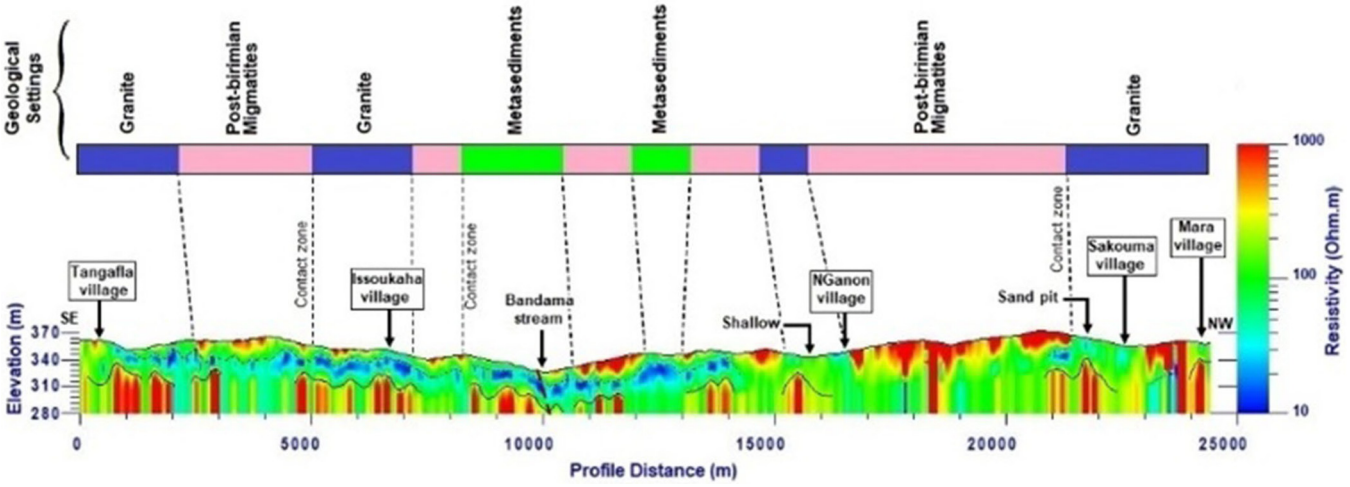

Fig. 8. Pseudo 2D resistivity section with main geological features. The black dashed line corresponds to the bottom of the indured saprolite. The saprolite and fissured zone layers are contained within the blue to green horizons. The solid black line is the interface between the fissured-rock zone and the basement. The red dashed lines indicate extrapolated tectonic faults.

In a large scale hard-rock aquifer conceptual model, the electrical resistivity is expected to decrease with depth as the water content increases, as in the study of Krivochieva and Chouteau (2003) done in Mexico integrating Time Domain Electromagnetic Method (TDEM) and Magnetotelluric Method (MT). In the upper compartment of the saprolite, we have many variations of the electrical resistivity between 10 and 10^3 Ω.m. We interpreted the low electrical resistivity zones as areas with high water content such as along the two main tectonic faults, the geological contacts, below the floodable area and the sand pit, and around the Bandama stream.

The saprolite exhibit electrical properties arising from changes in the degree of weathering and mineralogical composition of the constituent material in the zone. The saprolite layer lithology shows high heterogeneity in its composition varying from gravel to clay (see upper part of the lithologs given in Figures 4 to 7). The hydraulic conductivity is consequently variable. However, this saprolite layer presents a significant water retention capacity and plays a major role in the storage role of the aquifer. This was confirmed by the study of Legchenko *et al.* (2006) carried out in southern India with the MRS method.

The traditional hand dug wells of villages may catch water when reaching low electrical resistivity zones as visible under Tangafla, Issoukaha and Sakouma between 9 and 16 m depth (Fig. 8). It is known that the shallow wells in NGanon are problematic, dry most of the year. Indeed, for the concerned wells, we noticed on the surface of this area an indurated ferruginous crust extending over several kilometers square, typical of the region north of Ivory Coast. This layer is so hard that it prevents the digging of seedbeds to grow crops and the infiltration of water. Its lateral extension is correlated to the upper high electrical resistivity layer (red on Fig. 8) visible on most of the 24.4-km long profile, except on areas where we interpreted water infiltration zones.

Below the saprolite layer, we determined a fissured-rock layer overlying the bedrock. The fissured-rock layer is characterized as a mix of sub-horizontal and sub-vertical fissures in many studies conducted in Burkina Faso by Koussoubé *et al.* (2000), in India by Dewandel *et al.* (2006), in Zimbabwe by Houston and Lewis (1988), in France by Durand *et al.* (2006), and in Ouganda by Howard *et al.* (1992). Most of the water inflows are detected in the fissured horizon in the deep boreholes leading to high productivity in these wells (up to 10 m^3/h). Maréchal *et al.* (2004) conducted detailed hydrodynamic properties characterization of the fissured-rock zone of the hard-rock aquifer in India showing a permeability of 10^{-8} m/s in this zone, to be compared to10^{-4} m/s in the bedrock. Indeed the underlying massive hard-rock has very low water storage capacity and permeability.

The aquifer is characterized in our study by a relatively low electrical resistivity layer which allows us to follow its lateral depth and thickness variations. Finally, we notice in Figure 8 that our profile can be separated into two parts. In the SE first 15 km, the saprolite layer presents many heterogeneities in the electrical resistivity distribution and its interface with the fissured-rock zone is more detailed than in the NW last 10 km. The major tectonic faults might be responsible for these differences.

6 Conclusion

The study indicates that multifrequency EM method for geoelectrical resistivity imaging allow to identify the horizontal layers recognized in the basement aquifer, with the existence of the indured lateritic layer in particular. This method is also sensitive to vertical features such as faults, fractures and vertical contacts as well as near-surface lithological features which may have implications for hydrogeological considerations.

This study has contributed to better understand the geometry of the hard-rock aquifer in the white Bandama upstream watershed. The multifrequency EM method allows for non-invasive geophysical surface prospection able to provide rapid, dense and low cost data coverage that can be very useful for groundwater investigation in hard-rock context, especially when presenting very little EM noise. Adding the information obtained from lithologs as well as the geology of the area, the method is efficient to locate water reservoirs, implement evidences of deformations that affect the base, but not the groundwater level itself (water table on charge). The method is effective for identifying infiltration and recharging poles such as the river and fault zones that can affect the whole cuirass and build drains recharge of the aquifer. The electrical resistivity distributions derived from the EMS in the basin show the presence of a laterally fissured-rock layer, with water inflows, located in between the saprolite layer and the bedrock. This fissured-rock zone constitutes the main aquifer unit with thicknesses ranging from 15 to 30 m, and may constitute the captured zone for boreholes. Clearly, the integration of EMS data with borehole existing logs is advantageous to reduce ambiguity and uncertainty inherent to both of them. Our research work illustrates that the joint use of lithologs, geology and EM data inversion is promising for improving aquifer characterizations and to assist the construction of conceptual hydrogeological models.

Acknowledgements. Boreholes data were made available thanks to the library of the ministère des Infrastructures économiques, Direction technique de l'hydraulique in Korhogo, Ivory Coast. Many thanks to the staff of this office for their support and assistance for the field surveys. International Foundation for Science/Islamic Development Bank (IDB)'s partial funding was greatly appreciated.

References

Ahmed S, Sankaran S, Gupta CP. 1995. Variographic analysis of some hydrogeological parameters: use of geological soft data. *Journal Environmental Hydrology* 3(2): 28–35.

Beard L, Nyquist JE. 1998. Simultaneous inversion of airborne electromagnetic data for resistivity and magnetic permeability. *Geophysics* 63: 1556–1564. https://doi.org/10.1190/1.1444452.

Chave AD, Constable S, Edwards RN. 1991. Electrical exploration methods for the seafloor. In: Electromagnetic Methods in Applied Geophysics: volume 2, Applications, Part A and B. Society of Exploration Geophysicists. https://doi.org/10.1190/1.9781560802686.ch12.

Chilton PJ, Foster SSD. 1995. Hydrogeological characterisation and water-supply potential of basement aquifers in tropical Africa. *Hydrogeol J* 3: 36–49.

Dewandel B, Lachassagne P, Wyns R, Maréchal JC, Krishnamurthy NS. 2006. A generalized 3-D geological and hydrogeological conceptual model of granite aquifers controlled by single or multiphase weathering. *J Hydrol* 330: 260–284. https://doi.org/10.1016/j.jhydrol.2006.03.026.

Durand V, Deffontaines B, Leonardi V, Guerin R, Wyns R, de Marsily G, *et al.* 2006. A multidisciplinary approach to determine the structural geometry of hard-rock aquifers. Application to the Plancoet migmatitic aquifer (NE Brittany, W France). *Bull Soc Geol Fr* 177: 227–236. https://doi.org/10.2113/gssgfbull.177.5.227.

Dutta S, Krishnamurthy NS, Arora T, Rao VA, Ahmed S, Baltassat JM. 2006. Localization of water bearing fractured zones in a hard-rock area using integrated geophysical techniques in Andhra Pradesh, India. *Hydrogeol J* 14: 760–766. https://doi.org/10.1007/s10040-005-0460-7.

Farquharson CG, Oldenburg DW, Routh PS. 2003. Simultaneous 1D inversion of loop-loop electromagnetic data for magnetic susceptibility and electrical conductivity. *Geophysics* 68: 1857–1869. https://doi.org/10.1190/1.1635038.

Fraser DC. 1978. Resistivity mapping with an airborne multi coil electromagnetic system. *Geophysics* 43: 144–172.

Frischknecht FC, Labson VF, Spies BR, Anderson WL. 1991. Profiling methods using small sources. In: Nabighian MN, ed. Electromagnetic Methods in Applied Geophysics: volume 2, Applications, Part A and B. Society of Exploration Geophysicists, pp. 105–270.

Géomines. 1982. Inventaire hydrogéologique appliqué à l'hydraulique villageoise. Carte de Korhogo, cahier n° 6. République de Côte d'Ivoire: ministère des Travaux publics et des Transports, Direction centrale de l'hydraulique, 44 p.

Guillemoteau J, Sailhac P, Boulanger C, Trules J. 2015. Inversion of ground constant offset loop-loop electromagnetic data for a large range of induction numbers. *Geophysics* 80: 11–21. https://doi.org/10.1190/geo2014-0005.1.

Holland M, Witthüser KT. 2011. Evaluation of geologic and geomorphologic influences on borehole productivity in crystalline bedrock aquifers of Limpopo Province, South Africa. *Hydrogeol J* 19: 1065–1083. https://doi.org/10.1007/s10040-011-0730-5.

Houston JFT, Lewis RT. 1988. The Victoria Province drought relief project, II Borehole yield relationships. *Ground Water* 26: 418–426.

Howard KWF, Hughes M, Charlesworth DL, Ngobi G. 1992. Hydrogeologic evaluation of fracture permeability in crystalline basement aquifers of Uganda. *Appl Hydrogeol*. https://doi.org/10.1007/s100400050029.

Huang H, Fraser DC. 1996. The differential parameter method for multifrequency airborne resistivity mapping. *Geophysics* 61: 100–109. https://doi.org/10.1190/1.1574674.

Interpex. 2006. IX1D., v3 Tutorials. Golden, CO: Interpex Limited.

Karous M, Hjelt SE. 1983. Linear filtering of VLF dip-angle measurements. *Geophys Prospect* 31(5): 782–794. https://doi.org/10.1111/j.1365-2478.1983.tb01085.x.

Khalil MA, Santos FM. 2010. Comparative study between filtering and inversion of VLF-EM profile data. *Arab J Geosci* 4(1–2): 309–317. https://doi.org/10.1007/s12517-010-0168-4.

Koussoubé Y, Savadogo AN, Nakolendoussé S, Bazié P. 2000. Efficience de trois méthodes géophysiques d'investigation latérale dans l'identification de contacts géologiques entre des formations du Protérozoïque inférieur du Burkina Faso. *Revue PANGEA* (33/34): 49–60.

Krivochieva S, Chouteau M. 2003. Integrating TDEM and MT methods for characterization and delineation of the Santa Catarina aquifer (Chalco Sub-Basin, Mexico). *J Appl Geophys* 52: 23–43. https://doi.org/10.1016/S0926-9851(02)00231-8.

Lachassagne P, Wyns R, Bérard P, Bruel T, Chéry L, Coutand T, *et al.* 2001. Exploitation of high-yields in hard-rock aquifers: Down-scaling methodology combining GIS and multicriteria analysis to delineate field prospection zones. *Ground Water* 39: 568–581.

Lachassagne P, Wyns R, Dewandel B. 2011. The fracture permeability of hard-rock aquifers is due neither to tectonics, nor to unloading, but to weathering processes. *Terra Nov* 23: 145–161. https://doi.org/10.1111/j.1365-3121.2011.00998.x.

Legchenko A, Descloitres M, Bost A, Ruiz L, Reddy M, Girard JF, *et al.* 2006. Resolution of MRS applied to the characterization of hard-rock aquifers. *Ground Water* 44: 547–554. https://doi.org/10.1111/j.1745-6584.2006.00198.x.

Maréchal JC, Dewandel B, Subrahmanyam K. 2004. Use of hydraulic tests at different scales to characterize fracture network properties in the weathered-fractured layer of a hard-rock aquifer. *Water Resour Res* 40: 1–17. https://doi.org/10.1029/2004WR003137.

McNeill JD. 1990. Use of electromagnetic methods for groundwater studies. In: Ward SH, Society of Exploration Geophysicists, eds. Geotechnical and Environmental Geophysics. Tulsa OK, USA: Society of Exploration Geophysicists, pp. 191–218. https://doi.org/10.1190/1.9781560802785.ch7.

Palacky GJ, West GF. 1991. Airborne electromagnetic methods. In: Nabighian MN, ed. Electromagnetic methods in applied geophysics. Society of Exploration Geophysicists, pp. 811–880. https://doi.org/10.1190/1.9781560802686.ch10.

Schamper C, Rejiba F. 2011. 1D Inversion of multi-component and multifrequency low-induction number EM device (PROMIS®) for near-surface exploration. *PIERS ONLINE* 7: 126–130.

Schamper C, Rejiba F, Guérin R. 2012. 1D single-site and laterally constrained inversion of multifrequency and multicomponent ground-based electromagnetic induction data — Application to the investigation of a near-surface clayey overburden. *Geophysics* 77: WB19–WB35. https://doi.org/10.2529/PIERS100918093750.

Sinha AK. 1990. Interpretation of ground VLF-EM data in terms of inclined sheet-like conductor models. *Pure Appl Geophys PAGEOPH* 132: 733–756. https://doi.org/10.1007/BF00876817.

Tabbagh A, Bendritter Y, Andrieux P, Decriaud JP, Guerin R. 1991. VLF resistivity mapping and verticalization of the electric field. *Geophys Prospect* 39(8): 1083–1097. https://doi.org/10.1111/j.1365-2478.1991.tb00360.x.

Vouillamoz JM, Lawson FMA, Yalo N, Descloitres M. 2014. The use of magnetic resonance sounding for quantifying specific yield and transmissivity in hard-rock aquifers: the example of Benin. *J Appl Geophys* 107: 16–24. https://doi.org/10.1016/j.jappgeo.2014.05.012.

Wyns R, Baltassat J-M., Lachassagne P, Legchenko A, Vairon J, Mathieu F. 2004. Application of proton magnetic resonance soundings to groundwater reserve mapping in weathered basement rocks (Brittany, France). *Bull Soc Geol Fr* 175: 21–34. https://doi.org/10.2113/175.1.21.

Yadav GS, Singh SK. 2007. Integrated resistivity surveys for delineation of fractures for ground water exploration in hard-rock areas. *J Appl Geophys* 62: 301–312. https://doi.org/10.1016/j.jappgeo.2007.01.003.

Zhang Z, Routh PS, Oldenburg DW, Alumbaugh DL, Newman GA. 2000. Reconstruction of 1-D conductivity from dual-loop EM data. *Geophysics* 65: 492–501. https://doi.org/10.1190/1.1444743.

Cite this article as: Ouedraogo M, Pessel M, Durand V, Saintenoy A, Kamagate B, Savane I. 2022. Multifrequency electromagnetic method for the hydrogeophysical characterization of hard-rock aquifers: the case of the upstream watershed of White Bandama (northern Ivory Coast), *BSGF - Earth Sciences Bulletin* 193: 11.